Production of high transient heat and particle fluxes in a linear plasma device

Production of high transient heat and particle fluxes in a linear plasma device

G. De Temmerman,[a] J. J. Zielinski, H. van der Meiden, W. Melissen, and J. Rapp
FOM Institute for Plasma Physics Rijnhuizen, Association EURATOM-FOM, Trilateral Euregio Cluster, P.O. Box 1207, 3430 BE Nieuwegein, The Netherlands

(Received 27 April 2010; accepted 11 August 2010; published online 27 August 2010)

We report on the generation of high transient heat and particle fluxes in a linear plasma device by pulsed operation of the plasma source. A capacitor bank is discharged into the source to transiently increase the discharge current up to 1.7 kA, allowing peak densities and temperature of 70 $\times 10^{20}$ m^{-3} and 6 eV corresponding to a surface power density of about 400 MW m^{-2}. © *2010 American Institute of Physics*. [doi:10.1063/1.3484961]

Plasma-material interactions represent one of the key research areas for international thermonuclear experimental reactor (ITER). In a tokamak, power from the core plasma has to be exhausted by the plasma-facing components, mainly in the divertor area, where the plasma is neutralized and pumped away. In ITER, the steady-state heat load onto the divertor plates will be about 10 MW m^{-2}.[1] In addition, the very high localized heat fluxes during mitigated edge localized modes (ELMs) (2–4 GW m^{-2} for 0.5–1 ms) and represent a serious concern for the lifetime of the plasma-facing components,[2] because of the expected ELM frequency of up to 40 Hz.

To date, no tokamak can reach the heat loads expected during ITER ELMs, and laboratory simulation experiments are carried out using electron[3] or plasma guns,[4] or intense lasers aiming at reproducing relevant heat fluxes and timescales.[5] In ITER, however, the divertor plasma-facing materials (PFMs) will be exposed to both the steady state detached divertor plasma and the intense heat and particle fluxes during ELMs. Such a situation will lead to synergistic effects which might strongly affect the material damage threshold, as was observed during simultaneous plasma and laser irradiation of tungsten,[5] and which cannot be adequately reproduced in current experiments.

The Pilot-PSI linear device produces plasma parameters ($n_e \sim 0.1-10\times 10^{20}$ m^{-3}, $T_e \sim 0.2-5$ eV) relevant to the study of steady-state plasma-surface interactions in the ITER divertor.[6,7] In parallel, to simulate ELM-like conditions, a capacitor bank (5×135 μF, 200 J) is connected to the plasma source and discharged in the plasma source to transiently increase the input power. The pulse duration is about 750 μs. This allows the superimposition of a high transient heat and particle pulse to the steady-state plasma. Peak discharge currents of about 1.7 kA have been generated, corresponding to a peak input power of about 300 kW only limited by the stored energy in the capacitor bank. The plasma source was modified to accommodate the high heat fluxes generated during such pulses. The modified source consists of a stack of six water-cooled 6 mm thick copper plates with 8 mm diameter channel. The cathode is a 6.4 mm diameter tungsten rod. In addition, in order to maintain a high enough pressure in the plasma source, hydrogen flows of up to 10 slm (standard liters per minute) were used.

The plasma parameters are measured by means of a Thomson scattering (TS) system[8] located 17 mm in front of the plasma exposed target. The magnetic field, the trigger to the capacitor bank and the Thomson scattering system were synchronized in time with accuracy better than 1 μs to ensure a reproducible time delay between every step of the sequence. In order to measure the evolution of the electron temperature and density during the pulse, the delay time between the capacitor bank trigger and the Thomson system was varied. Each profile was averaged over several measurements to improve the statistics. Figure 1 shows the time evolution of

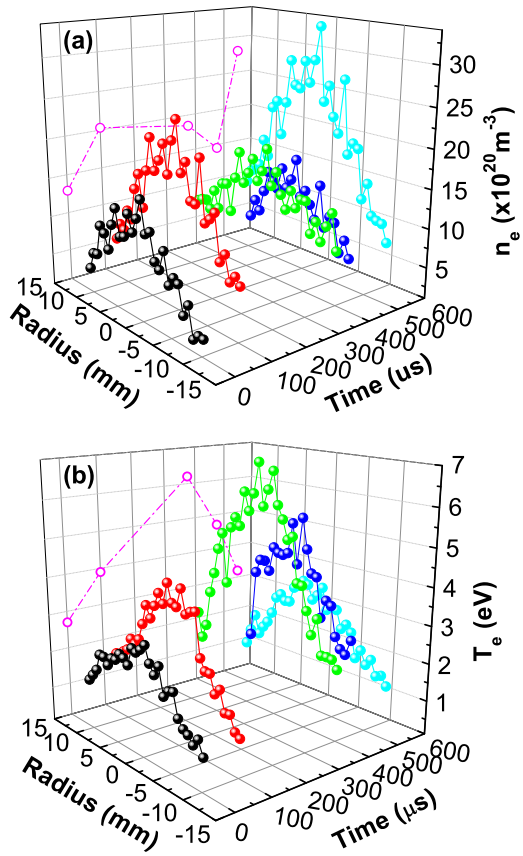

FIG. 1. (Color online) Time evolution of (a) electron density and (b) electron temperature profiles obtained for a discharge current of 1.7 kA and a magnetic field of 0.8 T. The temporal evolution of the peak temperature and density values, obtained from a fit of the measured profiles with a Gaussian curve, is indicated with open symbols.

[a]Electronic mail: g.c.temmerman@rijnhuizen.nl.

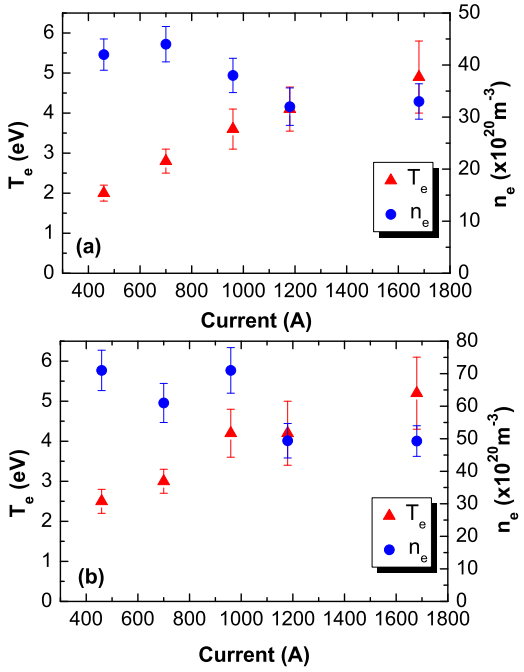

FIG. 2. (Color online) Peak values of electron density and temperature as a function of the peak discharge current for a fixed gas flow and magnetic field values of (a) 0.8 T and (b) 1.6 T.

electron temperature and density profiles obtained for a discharge current of 1.7 kA and a magnetic field of 0.8 T. The plasma exposed target was a 2 cm diameter polycrystalline tungsten disk, and was kept at floating potential during the experiments. The time evolution of the surface temperature during the pulse was monitored by a fast infrared camera (Santa Barbara Focal Plane, SBFB 125) which measures IR radiation in the wavelength range 4.5–5 μm. The framerate of the camera was set to 10 kHz in a subarray mode (128 $\times$8 pixels).

The discharge current was varied from 400 A to 1.7 kA, by varying the capacitor charge. During a pulse, the discharge voltage remains almost constant ($\sim$−170 V), so that the increase in input power is mainly driven by the increased discharge current. Under those conditions, the peak electron temperature and density varied from 2 to 6 eV and 10–70 $\times 10^{20}$ m^{-3}, respectively. Figure 2 shows the peak values of T_e and n_e for different discharge currents in the source and for magnetic field values of 0.8 T and 1.6 T, respectively. The hydrogen gas flow (6 slm) and the steady-state discharge current (175 A) were kept constant. For both values of the magnetic field, a slight decrease in the electron density (about 20%) is observed with increasing discharge currents, while the electron temperature increases by a factor 2.5 between 400 A and 1.7 kA, to values up to 5 eV. The electron density increases by about 50% when the magnetic field is increased from 0.8 to 1.6 T [Fig. 2(b)]. For a given gas flow and magnetic field, an increase in the input power is mainly converted to an increase in the electron temperature i.e., plasma heating. In parallel, a broadening of the plasma beam is observed during the plasma pulse. While the full width at half maximum (FWHM) of the density profile is about 15 mm before the actual pulse, the beam width increases to about 21.3 mm at the peak current, for a magnetic field of 0.8 T, and to about 18.7 mm at 1,6 T.

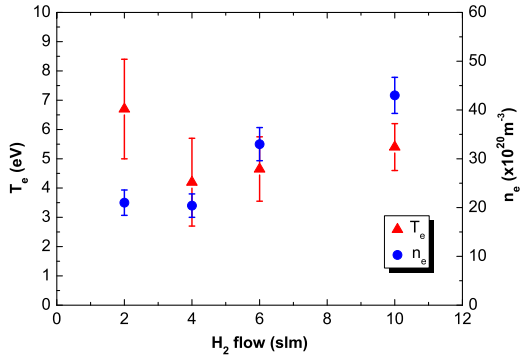

FIG. 3. (Color online) Peak values of electron density and temperature with different hydrogen gas flows, for a constant discharge current of 1.7 kA and magnetic field of 0.8 T.

Figure 3 shows the influence of the hydrogen gas flow on the peak temperature and density for a magnetic field of 0.8 T and a peak current of 1.7 kA. The electron density increases with the input gas flow, from 21×10^{20} m^{-3} for 2 slm to 43×10^{20} m^{-3} for 10 slm. The electron temperature is maximum for the lowest gas flow ($\sim$6.7 eV) and decreases sharply from 2 to 4 slm. A slight increase in T_e from 4.2 to 5.4 eV is then observed for increasing gas flow from 4 to 10 slm.

The time evolution of the electron temperature and density profiles during the plasma pulse are shown in Fig. 1. The temporal evolution of the peak temperature and density values, obtained from a fit of the measured profiles with a Gaussian curve, are also indicated in Fig. 1 with open symbols. During the pulse the electron density reaches its maximum after about 100 μs and remains almost constant until 375 μs [Fig. 1(a)], and then decreases at 475 μs. Surprisingly, the density increases abruptly at the end of the pulse and reaches values higher than those obtained during the pulse. On the other hand, the electron temperature [Fig. 1(b)] rises during the pulse and reaches a maximum at t =375 μs and decreases after that point. The post-pulse density rise is attributed to outgassing of trapped hydrogen from the target caused by the high surface temperature during a pulse (up to 1700 C) which is higher than the temperature at which complete desorption of deuterium from tungsten is observed.[9] Comparison of the temporal evolution of the surface temperature and of visible emission from the plasma using a fast visible camera with a framerate of 10 kHz, have indeed shown that the visible emission peaked around 200–300 μs later than the surface temperature, the latter corresponding to the peak temperature/density described in Fig. 1. The time delay between both measurements is in good agreement with the delay between the peak electron temperature and the time of the postpulse density rise (Fig. 1). The surface temperature rise time during a pulse is in the range 300–500 μs which is comparable with the rise time observed during Type-I ELMs in the JET tokamak.[2]

The peak surface heat flux during a pulse has been determined by two methods. The THEODOR code[10] has been used to calculate the heat flux profile along the target from the temporal evolution of the surface temperature during a pulse. For comparison, the surface heat flux has also been estimated from the Thomson scattering measurements by calculating the sheet heat transmission factor following the method described in.[11] The ion velocity at the sheath edge is

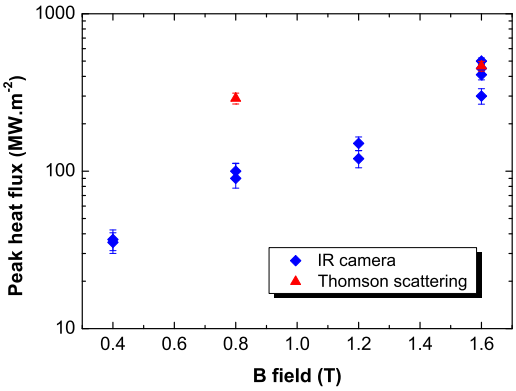

FIG. 4. (Color online) Peak power density on the plasma exposed target as a function of the magnetic field for a discharge current of 1.7 kA.

assumed to be the ion sound speed and the electron density at the sheath edge is assumed to be half of the upstream density (measured by the TS system). Surface recombination of hydrogen atoms is taken into account. Figure 4 shows the peak heat flux during a pulse as a function of the magnetic field. Evidently, the peak power density increases strongly with the magnetic field. Results from the TS data and infrared measurements are in good agreement for 1.6 T. As described above, the plasma density increases with the magnetic field, by about 50% from 0.8 to 1.6 T while T_e remains relatively unchanged, although the IR measurements indicate a factor 3 variation in the heat flux between those two field values. Since the gas pressure in the vessel is relatively high ($\sim$10 Pa) at the high gas flows investigated here, different loss mechanisms (like molecular assisted recombination) might contribute to such a discrepancy. With the existing setup, heat fluxes as high as 400 MW m^{-2} have been reached, only limited by the stored energy in the capacitor bank.

In summary, pulsed operations of the pilot-PSI plasma source allows producing high heat and particle fluxes superimposed on the divertor relevant steady-state plasma in a linear device. This represents a unique tool to study plasma-surface interactions during simultaneous irradiation by a high ion flux and transient heat/particles loads.

[1]R. A. Pitts, A. Kukushkin, A. Loarte, A. Martin, M. Merola, C. E. Kessel, V. Komarov, and M. Shimada, Phys. Scr. **T138**, 014001 (2009).
[2]A. Loarte, B. Lipschultz, A. S. Kukushkin, G. F. Matthews, P. C. Stangeby, N. Asakura, G. F. Counsell, G. Federici, A. Kallenbach, K. Krieger, A. Mahdavi, V. Philipps, D. Reiter, J. Roth, J. Strachan, D. Whyte, R. Doerner, T. Eich, W. Fundamenski, A. Herrmann, M. Fenstermacher, P. Ghendrih, M. Groth, A. Kirschner, S. Konoshima, B. LaBombard, P. Lang, A. W. Leonard, P. Monier-Garbet, R. Neu, H. Pacher, B. Pegourie, R. A. Pitts, S. Takamura, J. Terry, E. Tsitrone, and The ITPA Scrape-off Layer and Divertor Physics Topical Group, Nucl. Fusion **47**, S203 (2007).
[3]T. Hirai, S. Brezinsek, W. Kuehnlein, J. Linke, and G. Sergienko, Phys. Scr., T **111**, 163 (2004).
[4]I. E. Garkusha, N. I. Arkhipov, N. S. Klimov, V. A. Makhlaj, V. M. Safronov, I. Landman, and V. I. Tereshin, Phys. Scr. **T138**, 014054 (2009).
[5]S. Kajita, N. Ohno, S. Takamura, W. Sakaguchi, and D. Nishijima, Appl. Phys. Lett. **91**, 261501 (2007).
[6]G. J. van Rooij, V. P. Veremiyenko, W. J. Goedheer, B. de Groot, A. W. Kleyn, P. H. M. Smeets, T. W. Versloot, D. G. Whyte, R. Engeln, D. C. Schram, and N. J. Lopes Cardozo, Appl. Phys. Lett. **90**, 121501 (2007).
[7]W. A. J. Vijvers, C. A. J. van Gils, W. J. Goedheer, H. J. van der Meiden, D. C. Schram, V. P. Veremiyenko, J. Westerhout, N. J. Lopes Cardozo, and G. J. van Rooij, Phys. Plasmas **15**, 093507 (2008).
[8]H. J. van der Meiden, R. S. Al, C. J. Barth, A. J. H. Donné, R. Engeln, W. J. Goedheer, B. de Groot, A. W. Kleyn, W. R. Koppers, N. J. Lopes Cardozo, M. J. van de Pol, P. R. Prins, D. C. Schram, A. E. Shumack, P. H. M. Smeets, W. A. J. Vijvers, J. Westerhout, G. M. Wright, and G. J. van Rooij, Rev. Sci. Instrum. **79**, 013505 (2008).
[9]O. V. Ogorodnikova, J. Roth, and M. Mayer, J. Nucl. Mater. **313-316**, 469 (2003).
[10]A. Herrmann, W. Junker, K. Gunther, S. Bosch, M. Kaufmann, J. Neuhauser, G. Pautasso, Th. Richter, and R. Schneider, Plasma Phys. Contr. Fusion **37**, 17 (1995).
[11]P. C. Stangeby, *The Plasma Boundary of Magnetic Fusion Devices* (IOP, UK, 2000).